ELSEVIER

Journal of Biomechanics 34 (2001) 1125–1133

JOURNAL OF BIOMECHANICS

www.elsevier.com/locate/jbiomech
www.JBiomech.com

Fetal head moulding: finite element analysis of a fetal skull subjected to uterine pressures during the first stage of labour

R.J. Lapeer*, R.W. Prager

Department of Engineering, University of Cambridge, Cambridge CB2 1PZ, UK

Accepted 11 April 2001

Abstract

Fetal head moulding is a phenomenon which may contribute to satisfactory progress during delivery as it allows the fetal head to accommodate to the geometry of the passage. In contrast, excessive head moulding may result in cranial birth injuries and thus affect the infant shortly or even long after birth. One group of researchers in the past investigated the biomechanics of fetal head moulding from an engineering point of view and limited themselves to a static, linear model of the parietal bones. In this paper, we present a non-linear model of the deformation of a complete fetal skull, when subjected to pressures exerted by the cervix, during the first stage of labour. The design of the model involves four main steps: shape recovery of the fetal skull, the generation of a valid and compatible mesh for finite element analysis (FEA), the specification of a physical model and the analysis of deformation. Results of the analysis show good agreement with those obtained from clinical experiments on the quantitative assessment of fetal head moulding. The model also displays shapes after moulding which have been reported in previous studies and which are generally known in the obstetric and paediatric communities.

Keywords: Fetal head moulding; Finite element analysis; Shape modelling; Mesh generation; Labour forces

1. Introduction

In this paper we analyse the behaviour of the bony components of the fetal skull when subjected to pressures exerted by the cervix during the first stage of labour. The deformation of the skull bones and the fetal head in general, caused by external pressures during labour, is commonly referred to as fetal head moulding.

Several projects in the past (Geiger, 1993; Wischnik et al., 1993; Liu et al., 1996; Wischnik and Bohndorf, 1999) aimed to combine computer science and engineering to simulate the human birth process. Such a birth simulation is a useful diagnostic tool for obstetricians since it allows them to predict possible complications before the actual delivery. For instance, in the case of cephalo-pelvic disproportion,[1] the obstetrician could decide to perform an elective Caesarian section, rather than risking an emergency Caesarian section at delivery. A thorough understanding of the biomechanics of fetal head moulding would significantly improve the specificity[2] of the birth simulation as a diagnostic tool.

In paediatrics, a realistic model of fetal head moulding would be a major step towards the understanding of mechanical cranial birth injuries. Excessive moulding occurs when labour is prolonged or when contractions are too forceful or when there is a malposition of the fetal head or inept instrumental interference. Excessive displacements of the skull bones may cause bony lesions, dural membrane injury, intracranial hypertension, congestion of the Galenic venous system and direct injury of major intracranial vessels (Govaert, 1993).

McPherson and Kriewall investigated the bending properties of fetal cranial bone (McPherson, 1978; McPherson and Kriewall, 1980a) and used a static linear finite element (FE) model of the parietal bone to investigate fetal head moulding (McPherson, 1978; McPherson and Kriewall, 1980b). The research as presented in this paper extends their model to a

*Corresponding author.
E-mail address: rjal@eng.cam.ac.uk (R.J. Lapeer).

[1] Disproportion between the fetal head and the maternal pelvis, where the former is too large to pass through the latter.

[2] Specificity is the rejection rate of 'healthy' cases from treatment.

0021-9290/01/$ - see front matter
PII: S0021-9290(01)00070-7

non-linear static FE model of the deformation of a complete fetal skull.

2. Shape modelling and mesh generation

A finite element (FE) model of the mechanical behaviour of a fetal or newborn skull, which is subjected to labour forces, requires the accurate reconstruction of the shape of the fetal skull, followed by the creation of a valid, compatible mesh model. To reconstruct a 3D model of a bony biological organ, CT images are probably the best option because they exhibit a unique grey-value for bone tissue. However, for ethical, financial and political reasons, CT images of a newborn or fetus are scarcely available and if so, they are difficult to obtain. The same is true for MRI images, despite being less hazardous than CT, whilst 3D ultrasound images are too noisy to accurately recover the geometry. Therefore, we decided to reconstruct a shell-based surface model based on the laser scanning of the exact replica of a real fetal skull model as manufactured by ESP Ltd. A shell-based surface is justified since the bones of the cranial vault are thin compared to their in-plane dimensions (McPherson and Kriewall, 1980a).

The laser-scanning system operates according to the following principle (Linney et al., 1989): a beam of laser light is fanned out into a line and projected onto the object surface. When the line is viewed obliquely by a charge coupled device (CCD) camera it is curved, reflecting the shape of the surface at the intersection with the laser beam. To obtain a scan of the entire surface of the object, the latter is rotated on a platform. Individual data points can be recorded with a precision of less than 1 mm. The triangulation of the data points is straightforward because they form an ordered grid or matrix of points on the object surface. Shortcomings of the laser-scanning system include defects such as gaps caused at the locations where data points are *out of reach* (e.g. top and bottom of the skull when scanned in upright position), noise from interfering objects (e.g. the turntable) and surface patterns from vibration of the object during scanning. Therefore, several scans from different positions are acquired from which the most accurate parts are selected and registered (Lapeer, 1999). Fig. 1a shows the unconnected raw skull model, as a compound of patches from data acquisitions at several positions.

A front-based triangulation algorithm for surface interpolation using thin-plate splines was developed to interpolate missing parts of a surface, to create triangular meshes of arbitrary complexity and to optimise meshes to ensure optimal triangular aspect ratios. The algorithm is described in depth in Lapeer (1999, Chapter 3). Application of the algorithm to the incomplete skull as shown in Fig. 1a resulted in a final, compatible and optimised, triangular mesh model of the fetal skull as shown in Fig. 1b.

3. A biomechanical model of the first stage of labour

The processes involved in the expulsion of the fetus from the uterus and the resulting deformation of the head are complex. Therefore, we limited the model to

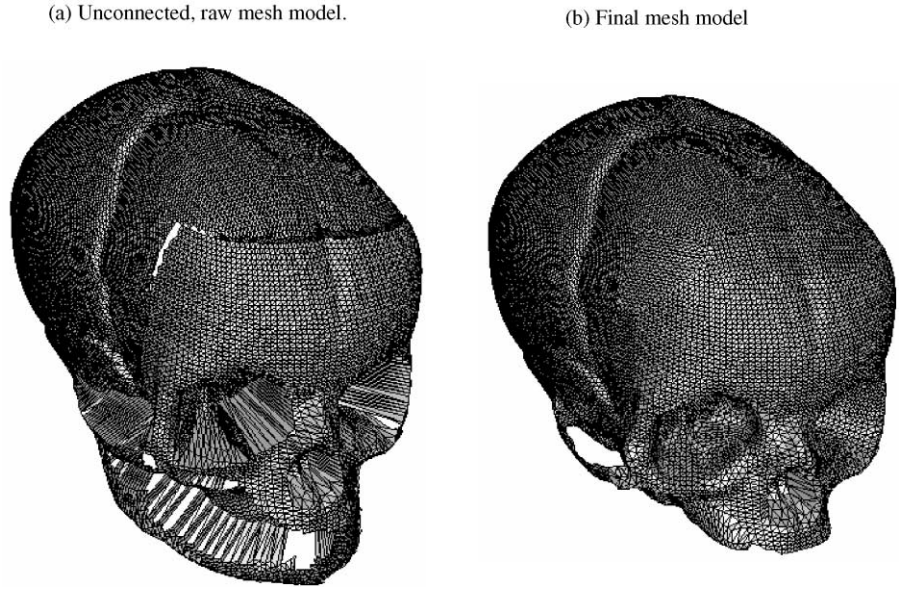

Fig. 1. Skull models before and after thin-plate spline surface interpolation and remeshing. (a) Unconnected, raw mesh model. (b) Final mesh model.

the first stage of labour when the fetal head is subjected to amniotic and cervical pressures.

3.1. The first stage of labour

The first stage of labour starts from the onset of *true* labour characterised by the increase of frequency and intensity of contractions which causes the fetus to be pressed against the lower uterine pole and the cervix to dilate. The first stage is completed when the cervix reaches full dilatation, which is conventionally taken as 10 cm (Friedman, 1954; Hendricks et al., 1970).

3.2. Intra-uterine pressure (IUP) and head-to-cervix pressure (HCP)

As early as 1861, attempts were made to assess forces in labour by inserting a spring measuring device in a pair of forceps. Subsequent investigations involved the insertion of balloons into the uterus via the vagina (Bell, 1972). More recently, more accurate measurements of the IUP (Turnbull, 1957) and HCP (Lindgren, 1960; Antonucci et al., 1997) during the first and second stages of labour were made, using intra-uterine catheters and pressure transducers. Since significant inter- and intra-observer variations exist amongst researchers, it is difficult to use these experimental results as a model for the pressure distribution during the first stage.

Bell (1972) suggested a theoretical model based on the assumptions that the lower pole of the fetal head is spherical (see Fig. 2). Equilibrium in the vertical direction then yields the equation (with $\phi_e = \pi/2$):

$$P_a \pi R^2 = \int_{\phi_0}^{\phi_e} P_r \cos\phi 2\pi r R \, d\phi. \quad (1)$$

The radial pressure (i.e. the HCP) is assumed to be proportional to the square of the radius of the head at all levels, an assumption based on experimental findings by (Lindgren, 1960):

$$P_r = C(r - r_i)^2 \quad (2)$$

After substitution of Eq. (2) into Eq. (1) (which eliminates the constant C) and working out we obtain

$$\Pi = \frac{P_r}{P_a} = \frac{6(\gamma - D_i)^2}{3(1 - D^4) - 8D_i(1 - D^3) + 6D_i^2(1 - D^2)}, \quad (3)$$

where P_r is the radial pressure or HCP, P_a the amniotic pressure or IUP, $\gamma = r/R$, the ratio of the local radius of contact and the greatest radius of the head, $D = \frac{r_0}{R} = \sin\phi_0$, the cervical dilatation as a fraction of the smallest radius of cervical contact and the greatest radius of the head, and $D_i = \frac{r_i}{R}$, the initial dilatation at the onset of labour.

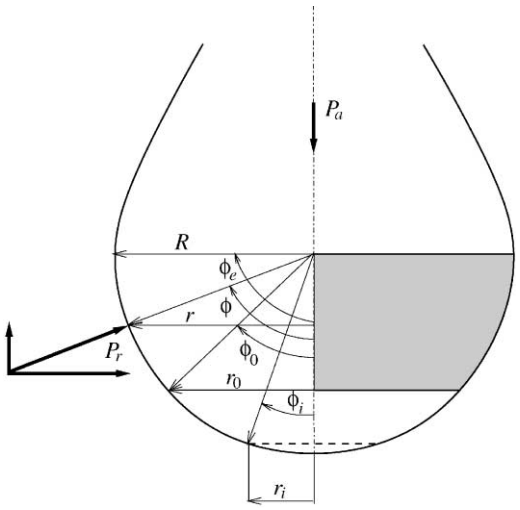

Fig. 2. Bell's idealised model: the spherical lower pole of the fetal head is in contact with the cervix. The dark-coloured patch shows the right half of the head-to-cervix contact area. P_r is the radial pressure (HCP), P_a is the amniotic pressure (IUP), R is the largest radius of the fetal head, r_i is the radius of initial dilatation and r_0 is the radius of the current dilatation.

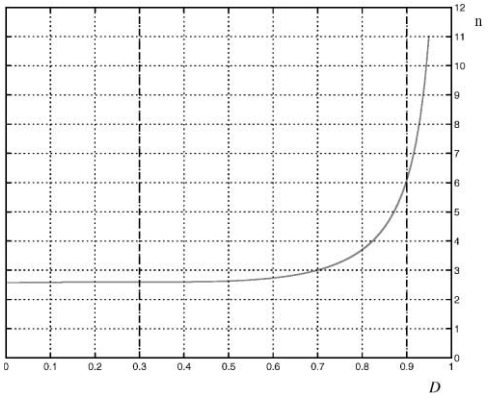

Fig. 3. Pressure ratio, Π, at the maximum diameter of the head as a function of cervical dilatation, D ($D_i = 0.3$).

Fig. 3 shows the pressure ratio, Π, at the largest diameter of the head (i.e. the sub-occipito bregmatic diameter) as a function of the dilatation, D. Assuming the IUP to be constant,[3] it is clear that a significant rise of the HCP occurs near dilatation $D > 0.7$.

3.3. Material properties

3.3.1. Material properties of fetal cranial bone

Fetal cranial bone is a very thin, non-homogeneous and highly curved material with a distinctly orientated

[3] Note that the IUP varies slowly in time between the basal pressure and the peak pressure. In this paper, only peak pressures (worst case) are considered which is justified by the fact that one period lasts typically about 2–3 min.

fiber pattern[4] (McPherson and Kriewall, 1980a). McPherson and Kriewall experimentally derived the elastic modulus of fetal cranial bone from three-point bending tests on 86 specimens obtained from six newborns, with an estimated gestational age ranging from 25 to 40 weeks (McPherson and Kriewall, 1980a). They found the material to be in-plane orthotropic with different elastic moduli in the tangential and radial directions relatively to the fibers.

Writing the constitutive equations of the stress, represented as a vector, $\boldsymbol{\sigma}$, as a function of the strain vector, $\boldsymbol{\varepsilon}$ (with elasticity matrix $\boldsymbol{E}$):

$$\boldsymbol{\sigma} = \boldsymbol{E}\boldsymbol{\varepsilon} \tag{4}$$

and in matrix form for an in-plane orthotropic material:[5]

$$\begin{bmatrix} \sigma_1 \\ \sigma_2 \\ \sigma_{12} \end{bmatrix} = \begin{bmatrix} \frac{E_1}{1-\nu_{12}\nu_{21}} & \frac{\nu_{12}E_2}{1-\nu_{12}\nu_{21}} & 0 \\ \frac{\nu_{21}E_1}{1-\nu_{12}\nu_{21}} & \frac{E_2}{1-\nu_{12}\nu_{21}} & 0 \\ 0 & 0 & \frac{E_1}{2(1+\nu_{12})} \end{bmatrix} \begin{bmatrix} \varepsilon_1 \\ \varepsilon_2 \\ 2\varepsilon_{12} \end{bmatrix}. \tag{5}$$

Based on experimental values of the elasticity moduli in two perpendicular directions, E_1 and E_2 as reported in McPherson and Kriewall (1980b), Poisson's ratio for tangential compression of adult cranial bone as an estimate for ν_{12} and reported in McElhaney et al. (1970), and the assumption that the in-plane shear stress components on perpendicular faces must be equal in magnitude (Crandall et al., 1978):

$$\nu_{21}E_1 = \nu_{12}E_2 \tag{6}$$

with $\nu_{12} = 0.22$, $E_1 = 3.860$ GPa and $E_2 = 0.965$ GPa, we obtain from Eq. (6): $\nu_{21} = 0.055$. Substitution of these values in Eq. (5) yields the elasticity matrix

$$\boldsymbol{E} = \begin{bmatrix} 3.907 & 0.215 & 0 \\ 0.215 & 0.977 & 0 \\ 0 & 0 & 1.582 \end{bmatrix}. \tag{7}$$

3.3.2. Material properties of fontanelles and sutures

For the fontanelles and sutures we adopted values as reported by Bylski et al. (1986) who investigated the material properties of fetal dura mater. They assumed the material to be homogeneous, isotropic, non-linearly elastic, incompressible and undergoing large deformation when subjected to a static load (hyperelastic). Assuming a Mooney–Rivlin model, the following material constants were reported for fetal dura mater:

$C_1 = 1.18$ MPa,

$C_2 = 0.295$ MPa.

[4] Unlike the homogeneous grain structure of adult cranial bone!

[5] Note that the derivation of the shear modulus, $G = 2(1 + \nu_{12})/E_1$, is based on the assumption that the material is in-plane isotropic rather than in-plane orthotropic (McPherson and Kriewall, 1980b).

Table 1
Original diameters and absolute diametral displacements (in mm) as reported by Sorbe and Dahlgren (1983) (columns 1 and 2), from a previous experiment by Lapeer and Prager and reported in Lapeer and Prager (1999) (columns 3 and 4), and from the current experiment (columns 5 and 6)

	S–D		L–P old		L–P new	
Diameter	Length	Displ.	Length	Displ.	Length	Displ.
MaVD	140.5	+1.90	129.3	+0.30	129.3	+1.43
OrOD	131.4	+0.10[a]	—	—	119.9	+1.85
OrVD	126.9	+2.20	119.3	+0.25	119.3	+1.24
OFD	134.0	+0.40[a]	—	—	119.7	+1.82
SOFD	—	—	—	—	113.2	−0.85
SOBD	117.1	−1.70	88.7	−1.07	88.7	−2.52
BPD	105.0	0.00	89.7	−0.21	89.7	−0.83

[a] Not statistically significant.

The anisotropic and viscoelastic behaviour, generally displayed by soft tissues (Fung, 1993) was ignored by the authors. This assumption was justified from research by Melvin et al. (1970) who reported that the general variability in the adult dura mater tissue tends to overshadow the anisotropic and viscoelastic effects.

3.3.3. Material properties of the skull base and maxilla

Adult cranial bone is a transversely (tangent to the skull surface) isotropic material (Wood, 1971). Material constants for the skull base and maxilla of the fetal skull have not been reported as yet. We will assume that the fetal skull base and maxilla are similar to adult cranial bone and adopt the values of Young's modulus, $E =$ 4.46 GPa, and Poisson's ratio, $\nu = 0.22$, for an adult skull, as reported by McElhaney (1973).

3.4. Validation of the model

Sorbe and Dahlgren (1983) investigated 319 vaginal deliveries. They used a photographic method to document the size of the infant's head, immediately postpartum and 3 days later. Six different diameters were measured: the biparietal diameter, BPD, the occipito-frontal diameter, OFD, the orbito-occipital diameter, OrOD, the suboccipito-bregmatic diameter, SOBD, the maxillo-vertical diameter, MaVD, and the orbito-vertical diameter, OrVD. A modified moulding index, MMI, was used based on Kriewall's moulding index MI (Kriewall et al., 1977):

$$\mathrm{MMI} = \frac{\mathrm{MaVD}^2}{\mathrm{BPD} \times \mathrm{SOBD}}. \tag{8}$$

They observed significant changes for the SOBD, OrVD and MaVD. These values are reported in Table 1. Fig. 7 shows the diameters and the anatomy of the fetal skull.

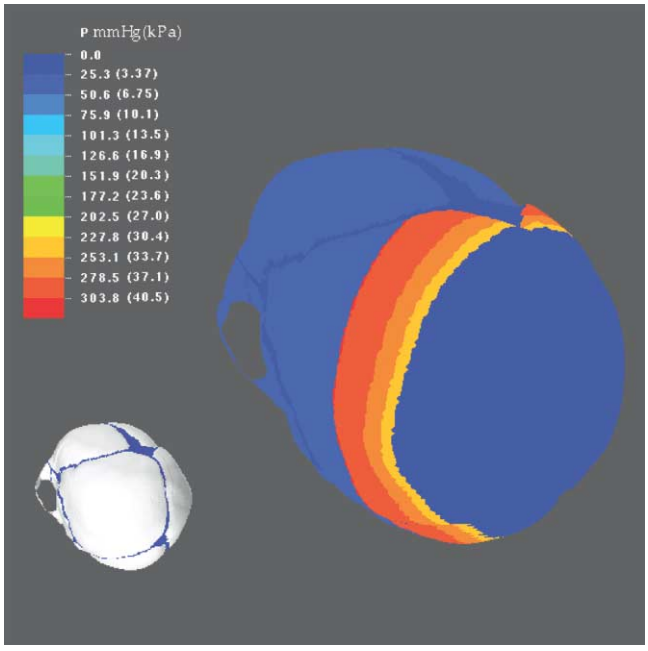

Fig. 4. Pressure distribution as exerted by the cervix and the amniotic fluid at dilatation, $D = 0.9$. The amniotic or intra-uterine pressure (IUP) is 50 mmHg, the initial dilatation, D_i, is 0.3. Note that there is no pressure exerted on the fontanelles and sutures.

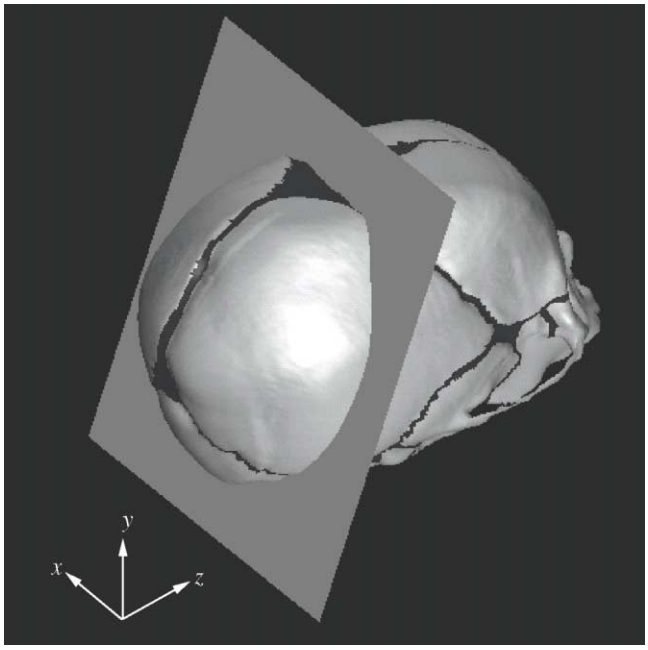

Fig. 5. Location of the sub-occipito bregmatic (SOB) plane, corresponding to an *occiput anterior vertex* presentation and the axis directions for the analysis of deformation of the fetal skull model.

4. Experiments

McPherson and Kriewall investigated the deformation of the parietal bones when subjected to a linearly varying HCP (McPherson, 1978; McPherson and Kriewall, 1980b). The finite element (FE) model they used contained 64 nodes and 63 first-order elements. The shape of the bones was derived from X-ray images of a fetal skull. Assuming linear geometry, they found diametral strains of around 1% for dilatation $D = 0.5$. Their experiment was validated in Lapeer (1999) with more accurate models of up to 10,000 second-order elements and diametral strains of more than 7% were found, though the shape after deformation corresponded with their findings.

The experiment described in this section involves the evaluation of the entire skull when subjected to the IUP and HCP. From Eq. (3) and Fig. 3 we saw that higher dilatations result in significantly higher HCPs. Experiments at different dilatations as reported in Lapeer (1999) showed that higher HCPs corresponded to higher degrees of moulding. Therefore, we will limit the experiment reported here to dilatation, $D = 0.9$.[6]

Fig. 4 shows the pressure distribution on the fetal skull calculated from the idealised model formalised in Eq. (3). Fig. 5 shows the sub-occipito bregmatic (SOB) plane. Below this plane, the cervix is in contact with the head, a configuration which corresponds to the most common presentation, the *occiput anterior vertex* presentation. Above the plane, the skull is subjected to the intra-uterine (amniotic) pressure. The skull model as shown in Fig. 1b was used. It contains 63,413 first-order, thin-shell, triangular elements.

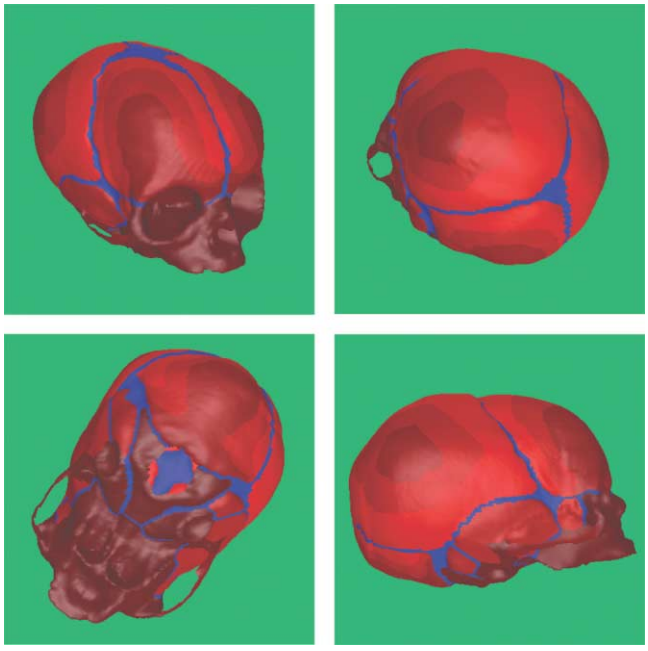

Fig. 6. Coloured fetal skull model: *red* colour is bone; *blue* colour are sutures/fontanelles. Darker *red* colours correspond to regions of higher thickness values (visualisation in Geomview 1.6.1; Phillips, 1996).

The geometry was further subdivided into different regions of different material properties. Fig. 6 shows this

[6] Note that for higher dilatations the model as formulated in Eq. (3) shows poor agreement with values reported from clinical experiments.

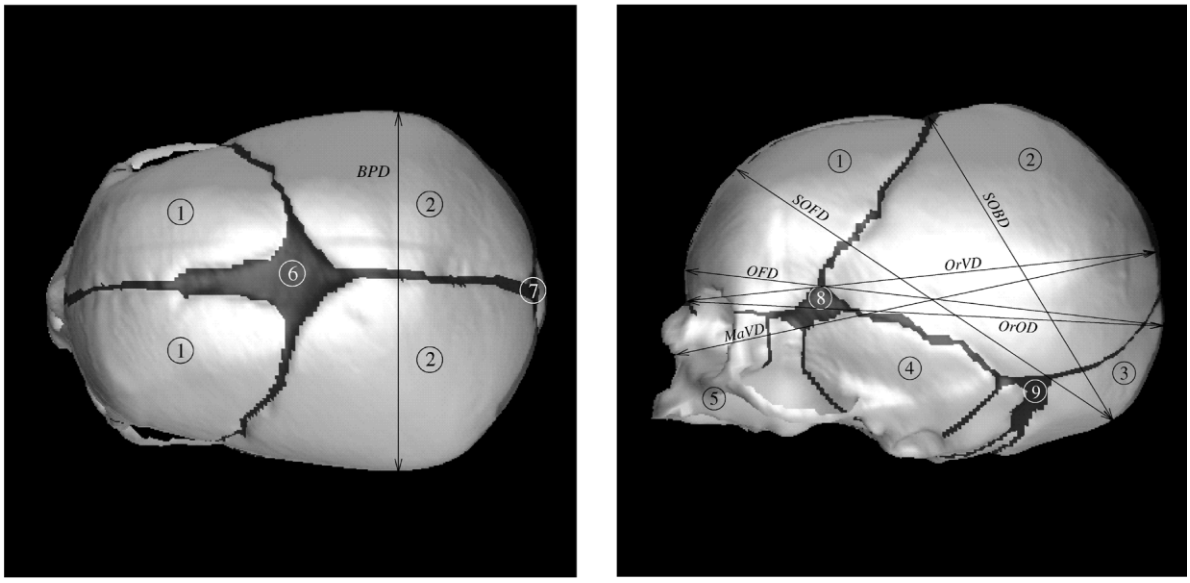

Fig. 7. Anatomy of the fetal skull and diameters for evaluation of fetal head moulding. 1 = frontal bone, 2 = parietal bone, 3 = occipital bone, 4 = temporal (squamosal) bone, 5 = skull base, 6 = anterior fontanelle, 7 = posterior fontanelle, 8 = sphenoidal fontanelle, 9 = mastoidal fontanelle (see text for explanation of the diameters).

subdivision represented by different colours. McPherson and Kriewall (1980b) discovered that the bones of the cranial vault, i.e. the parietal and frontal bones and the occipital bone, are thicker in their centres and become gradually thinner towards the outer edges. They subdivided the bones into three concentric regions emanating from the centre with average thicknesses of 0.89, 0.74 and 0.61 mm, respectively. These different regions are shown in Fig. 6 in different shades of red. The skull base and maxilla are coloured dark red and their thickness is set to 2 mm—an estimate based on the thickness of the palate of the fetal skull model. The fontanelles and sutures are coloured blue and have an average thickness of 0.57 mm as reported in Bylski et al. (1986). The material properties are set as specified in Eq. (7) and Sections 3.3.2 and 3.3.3.

Boundary conditions are met by three fully built-in nodes on the base of the skull to avoid rigid body translation and rotation. Additionally, three fully built-in nodes on the facial part of the skull are specified, to avoid rigid body rotation about the x-axis. A static analysis, assuming non-linear geometry, was performed using the ABAQUS FE software.

Fig. 7 shows the diameters for evaluation: MaVD, OrOD, OrVD, OFD, SOFD, SOBD, and BPD.

4.1. Results

Table 1 shows the original diameters and the diametral displacements in mm, as reported from the clinical experiment by Sorbe and Dahlgren (1983), from an earlier experiment as reported in Lapeer and Prager (1999) and from the current experiment.[7]

Table 2
The modified moulding index (MMI) for the biomechanical model of fetal head moulding and from clinical experiments by Sorbe and Dahlgren

	Before	After	% Moulding
S–D[a]	2.08	2.18	4.8
L–P new	2.10	2.23	6.2

[a] The MMIs from Sorbe and Dahlgren are averages and corrected to account for the skin

Table 2 shows the modified moulding index, MMI, for the clinical and the current experiment.

The percentage of moulding as shown in Table 2 is calculated from

$$\frac{\mathrm{MMI_a} - \mathrm{MMI_b}}{\mathrm{MMI_b}} \times 100, \tag{9}$$

where $\mathrm{MMI_b}$ and $\mathrm{MMI_a}$ are the modified moulding indices before and after moulding, respectively.

Table 3 shows the strains in %, for the clinical and the current experiment.

Finally, Fig. 8 shows the moulding of the fetal skull as predicted by the biomechanical model for frontal, lateral and top views, respectively.

[7] Note that the diametral lengths as reported in the current experiment are smaller than the reported values by Sorbe and Dahlgren because the latter include the skin. This discrepancy should make no difference to the corresponding values of the diametral displacements.

Table 3
Diametral strains (%) for the biomechanical model and corrected average diametral strains from Sorbe and Dahlgren (1983), for all diameters

	MaVD	OrOD	OrVD	OFD	SOFD	SOBD	BPD
S–D	+1.47	+0.08[a]	+1.85	+0.33[a]	—	−1.90	0.00
L–P new	+1.10	+1.63	+1.04	+1.52	−0.75	−2.84	−0.92

[a] Not statistically significant

5. Discussion

Comparing the clinical experimental data from Sorbe and Dahlgren (1983) and the results from our biomechanical model, relatively good agreement, both in terms of the *shape after deformation* as the *degree of deformation*, is shown. The correspondence in terms of deformation of the original shape is illustrated by the

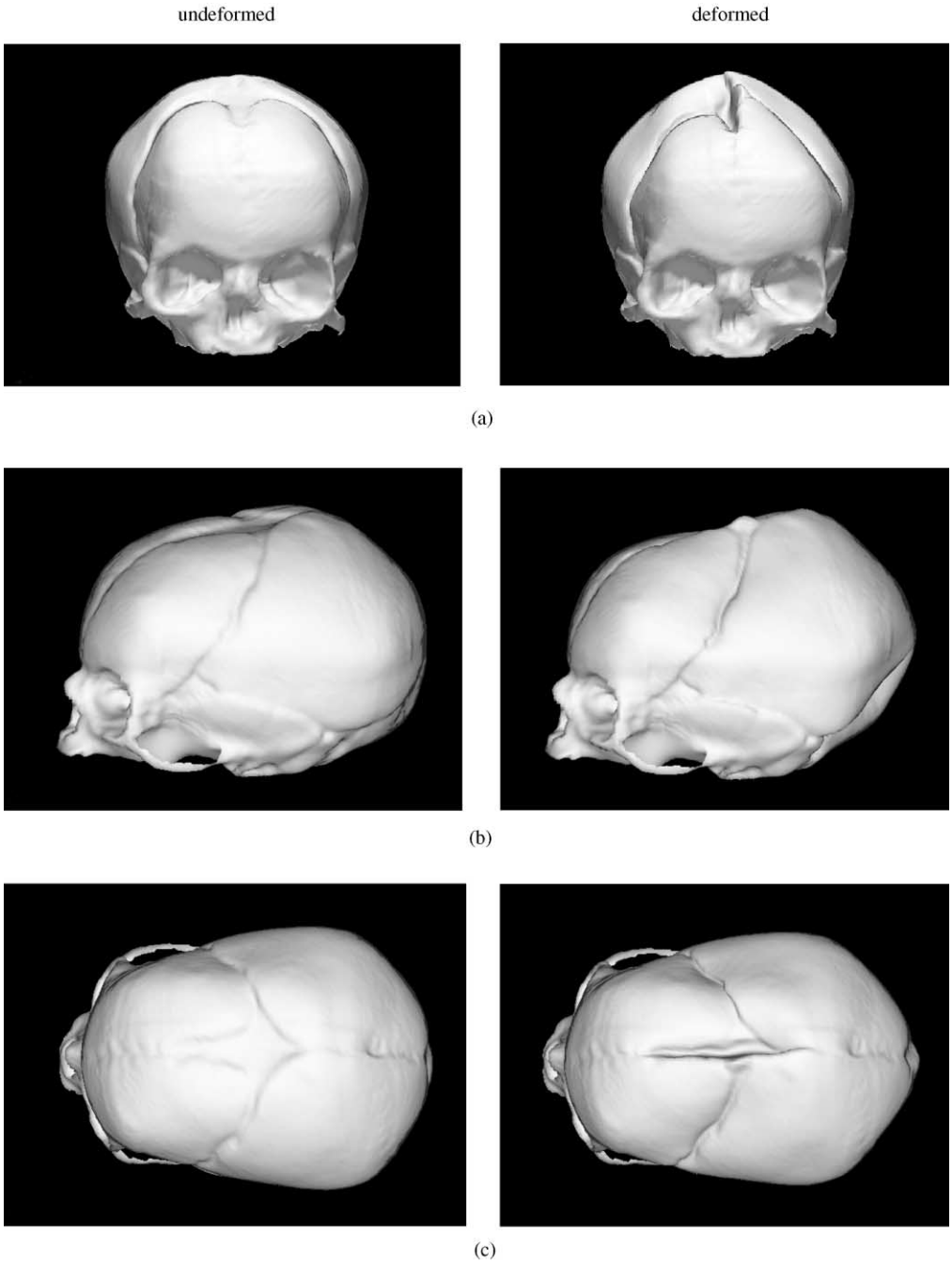

Fig. 8. Effects of the cervical and amniotic pressure during the first stage of labour on fetal head moulding—deformation magnification = 4. (a) frontal view, (b) lateral view, (c) top view.

elongation of the MaVD and the OrVD (positive diametral displacement) and the compression of the SOBD (negative diametral displacement) for the three experiments. The degree of deformation is much closer to Sorbe and Dahlgren's experimental values for the current (new) experiment than for the (old) experiment as reported in Lapeer and Prager (1999). The main distinction between these two models lies in the modelling of the material properties of the fontanelles and sutures. In the old model, properties of adult dura mater as reported in McElhaney (1973) were used. The material was assumed to be linearly elastic. In the current model, properties of fetal dura mater were used as reported in Bylski et al. (1986) and the material was assumed to be hyperelastic. It is however doubtful that the drastic change in the degree of deformation as compared to earlier results can be credited to a hyperelastic Mooney–Rivlin model with just two parameters. The true reason for displaying a higher (and more realistic) degree of deformation are probably the more realistic and smaller values of the two hyperelastic material constants, i.e. $C_1 = 1.18$ MPa and $C_2 = 0.295$ MPa, for fetal dura mater, as compared to the linear elastic constant, $E = 31.5$ MPa, for adult dura mater. The Mooney–Rivlin (MR) model, which was chosen at this stage for its simplicity, is inferior as a model for the soft tissue of fetal dura mater as compared to the Skalak, Tozeren, Zarda and Chien (STZC) model, which was illustrated in Bylski et al. (1986). The implementation of this model in future work is necessary for further assessment of the hyperelastic assumption. In general, the resulting deformations may though indicate that the stiffness of the fetal skull is very much dependent on the properties of the soft tissues.

A peculiar finding is that the BPD did not change in Sorbe and Dahlgren's experiments, whilst the authors' findings point to a small decrease of this diameter. This is however in agreement with McPherson's parietal bone test (McPherson, 1978) which reports a decrease of about 2% of the BPD.

The OrOD and OFD did not show statistically significant changes according to Sorbe and Dahlgren (1983) but the signs of the displacements are nonetheless in agreement with our findings. The SOFD was not reported in Sorbe and Dahlgren (1983) and showed a rather small negative displacement in our model.

The general shape deformations, as represented by the diametral changes, are visualised in Fig. 8. Figs. 8a and b show the lifting of the parietal bones. This suggests a decrease of the BPD which is illustrated in Figs. 8a and c. The latter figure shows the bulging of the anterior fontanelle because of the lifting of the parietal bones. This phenomenon also causes the area near the posterior fontanelle to move outwards in the negative z-direction (see Fig. 5) which results in an increase of the OFD, OrOD, MaVD and the OrVD. The lifting of the protuberance of the occipital bone results in the decrease of the SOBD.

Table 2 shows the MMI, for the experimental results from Sorbe and Dahlgren (1983) and from the new model. The latter shows a slightly higher degree of moulding. From Eq. (8) we see that the MMI is proportional to the square of the MaVD and inversely proportional to the product of the SOBD and BPD. For the experimental clinical model, the MaVD increases more than for the biomechanical model; however, the SOBD and BPD, decrease proportionally more for the latter, thus resulting in a higher MMI. Some caution has to be taken with the interpretation of the MMI because it does not include all diameters and its theoretical derivation, based on principal dimensions when the head is considered to exhibit the shape of an ellipsoid (Kriewall et al., 1977), is rather fragile.

Table 3 shows the strains which are in relatively good agreement, in terms of order of magnitude, between the models.

6. Conclusion

The biomechanical model of fetal head moulding as presented in this paper is a significant improvement compared to the earlier model of the parietal bones, suggested by McPherson and Kriewall (McPherson, 1978; McPherson and Kriewall, 1980b) and the more recent model, presented in Lapeer and Prager (1999). Despite the use of a relatively small number of parameters compared to the many involved in the birth process, and the potentially large variation within this small set of parameters, the model shows good agreement with clinical experiments, both in terms of *shape after deformation* and the *degree of deformation*. Moreover, the lifting of the parietal bones, is a commonly known phenomenon in the obstetric and paediatric communities and has previously been reported in Govaert (1993), Lapeer (1999) and McPherson and Kriewall (1980b).

The model as presented in this paper, allows us to evaluate the biomechanics of fetal head moulding in a quantitative fashion and continuously across the geometry. Therefore, it can be used in the obstetric field, to improve the sensitivity of a computerised birth simulation, aimed at the early diagnosis of possible complications during vaginal delivery. In the paediatric field, it can be applied to investigate mechanical cranial birth injuries as well as congenital malformations such as hydrocephalus.

Future improvements to the model should involve the analysis of variation of the different model parameters and their influence on head moulding. More accurate reconstruction of the geometry of the skull could be

obtained from computed tomography (CT) data. Acquisition of several such datasets would allow us to investigate the sensitivity of fetal skull moulding to variations in shape. Further investigations on the material properties as conducted by Bylski et al. (1986) and McPherson and Kriewall (1980a) may prove useful but again the ethical factor may pose a problem. More sophisticated measurements of the IUP and the HCP in both the first and second stage and possibly in conjunction with measurements of several diameters after delivery would significantly improve the accuracy of the physical model.

The actual IUP changes during time with a frequency of about 18–30 uterine contractions per hour (Lindgren, 1977). The current model was assumed to be static and based on peak pressures (worst case). The consideration of a more realistic quasi-static model may prove useful especially in conjunction with viscoelastic and plastic models of the bones of the cranial vault. A mechanical contact model of the underlying structures such as the female pelvis and the uterine tract, and consideration of the second stage of labour, may further improve the quantitative assessment of fetal head moulding.

Acknowledgements

Thanks are due to Dr. Robin Richards for the data acquisition of the fetal skull. The first author also wishes to thank Prof. J.C. Barbenel and Dr. T.J. Lu for their valuable comments and is grateful for the financial support provided by the EPSRC and the Cambridge European Trust.

References

Antonucci, M., Pitman, M., Eid, T., Steer, P., Genevier, E., 1997. Simultaneous monitoring of head-to-cervix forces, intrauterine pressure and cervical dilatation during labour. Medical Engineering Physics 19 (4), 317–326.

Bell, F., 1972. Biomechanics of human parturition: a fundamental approach to the mechanics of the first stage of labour. Ph.D. Thesis, University of Strathclyde, Glasgow.

Bylski, D., Kriewall, T., Akkas, N., Melvin, J., 1986. Mechanical behavior of fetal dura mater under large deformation biaxial tension. Journal of Biomechanics 19 (1), 19–26.

Crandall, S., Dahl, N., Lardner, T., 1978. An Introduction to the Mechanics of Solids. McGraw-Hill, Singapore.

Friedman, E., 1954. The graphic analysis of labor. American Journal of Obstetrics and Gynecology 68 (6), 1568–1575.

Fung, Y., 1993. Biomechanics: Mechanical Properties of Living Tissues, 2nd Edition. Springer, New York.

Geiger, B., 1993. Three-dimensional modeling of human organs and its application to diagnosis and surgical planning. Ph.D. Thesis, Ecole des Mines de Paris.

Govaert, P., 1993. Cranial Haemorrhage in the Term Newborn Infant. Mac Keith Press, Cambridge University Press, London.

Hendricks, C., Brenner, W., Kraus, G., 1970. Normal cervical dilatation pattern in late pregnancy and labor. American Journal of Obstetrics and Gynecology 106 (7), 1065–1082.

Kriewall, T., Stanley, J., McPherson, G., 1977. Neonatal head shape after delivery: an index of molding. Journal of Perinatal Medicine 5 (6), 260–267.

Lapeer, R., 1999. A biomechanical model of foetal head moulding. Ph.D. Thesis, University of Cambridge.

Lapeer, R., Prager, R., 1999. Finite element model of a fetal skull subjected to labour forces.. In: Taylor, C., Colchester, A. (Eds.), MICCAI'99, Lecture Notes in Computer Science, Vol. 1679. Springer, Berlin, pp. 1143–1155.

Lindgren, L., 1960. The causes of foetal head moulding in labour. Acta Obstetricia et Gynecologica Scandinavica 39, 46–62.

Lindgren, L., 1977. The influence of pressure upon the fetal head during labour. Acta Obstetricia Gynecologica Scandinavica 56 (4), 303–309.

Linney, A., Grindrod, S., Arridge, S., Moss, J., 1989. Three-dimensional visualization of computerized tomography and laser scan data for the simulation of maxillo-facial surgery. Medical Informatics 14 (2), 109–121.

Liu, Y., Scudder, M., Gimovsky, M., 1996. CAD Modeling of the birth process. Part II. In: Sieburg, H., Weghorst, S., Morgan, K. (Eds.), Health Care in the Information Age. IOS Press and Ohmsha, Burke, VA, pp. 652–666.

McElhaney, J., 1973. Dynamic characteristics of the tissues of the head. In: Kenedi, R. M. (Ed.), Perspectives in Biomedical Engineering, MacMillan Press, Ltd, London, pp. 215–222.

McElhaney, J., Fogle, J., Melvin, J., Haynes, R., Roberts, V., Alem, N., 1970. Mechanical properties of cranial bone. Journal of Biomechanics 3 (5), 495–511.

McPherson, G., 1978. Mechanical properties of fetal cranial bone and their influence on head molding in parturition. Ph.D. Thesis, The University of Michigan.

McPherson, G., Kriewall, T., 1980a. The elastic modulus of fetal cranial bone: a first step towards an understanding of the biomechanics of fetal head molding. Journal of Biomechanics 13 (1), 9–16.

McPherson, G., Kriewall, T., 1980b. Fetal head molding: an investigation utilizing a finite element model of the fetal parietal bone. Journal of Biomechanics 13 (1), 17–26.

Melvin, J., McElhaney, J., Roberts, V., 1970. Development of a mechanical model of the human head—determination of tissue properties and synthetic substitute materials. In: Proceedings of the Fourteenth STAPP Car Crash Conference. Society of Automotive Engineers, New-York, pp. 221–240.

Phillips, M., 1996. Geomview Manual—Version 1.6.1. The Geometry Center.

Sorbe, B., Dahlgren, S., 1983. Some important factors in the molding of the fetal head during vaginal delivery—a photographic study. International Journal of Gynaecology and Obstetrics 21 (3), 205–212.

Turnbull, A., 1957. Uterine contractions in normal and abnormal labour. American Journal of Obstetrics and Gynecology 64 (3), 321–333.

Wischnik, A., Bohndorf, K., 1999. Zur Prävention des menschlichen Geburtstraumas II. Mitteilung: Wissensbasierte Geburtsplanung und visualisierung mittels bildgebender Verfahren und PC-gestützter Simulation. Geburtshilfe und Frauenheilkunde 59 (2), 77–84.

Wischnik, A., Nalepa, E., Lehmann, K., Wentz, K., Georgi, M., Melchert, F., 1993. Zur Prävention des menschlichen Geburtstraumas I. Mitteilung: Die computergestützte Simulation des Geburtsvorganges mit Hilfe der Kernspintomographie und der Finiten-Element-Analyse. Geburtshilfe und Frauenheilkunde 53 (1), 35–41.

Wood, J., 1971. Dynamic response of human cranial bone. Journal of Biomechanics 4 (1), 1–12.